The application of strain energy density criterion to fatigue crack growth behavior of cracked components

M. Rashidi Moghaddam[a] M.R. Ayatollahi[a] F. Berto[b]

Abstract

The aim of this paper is to study the effects of specimen geometry on fatigue crack growth rate and fatigue life in cracked components by using a modified form of averaged strain energy density criterion. The modified criterion takes into account the first non-singular term of the Williams series expansion in addition to the classical stress intensity factors. Different samples are used to conduct high cycle fatigue experiments on Al 7075-T6. The fatigue behavior of cracked Al 7075-T6 samples is investigated experimentally and theoretically for the compact tension (CT), double cantilever beam (DCB) and Brazilian disc (BD) specimens. It is shown that the fatigue crack growth in these specimens is significantly geometry-dependent. The modified criterion can predict the fatigue crack growth rate and the fatigue life of the pre-cracked specimens well.

Keywords

Strain energy density
Fatigue crack growth
Geometry effects

1. Introduction

Cyclic loading can generate a fatigue damage mechanism in the structures leading to nucleation of a small crack, followed by crack growth, and ultimately to complete failure. The analysis of crack growth is one of the key problems in safety evaluation of industrial components subjected to cyclic loading. The rate of crack growth due to fatigue loading is commonly determined through experiments. There are also models to predict fatigue crack growth rate which are often based on phenomenological descriptions.

In high cycle fatigue region (i.e. under small scale yielding conditions), a correlation between the fatigue crack growth rate da/dN and the cyclic stress intensity factor (SIF) range ΔK_I was introduced by Parsi et al. [1] in 1961. According to the simplest form, commonly known as the Paris law, the relation between da/dN (for midrange fatigue crack growth rate) and ΔK_Ican be described by a power function as:

(1)dadN=C(ΔKI)m

where the material constants C and m are assumed to be independent of the specimen geometry. The equation in a double log plot gives a linear relation: $\log(da/dN) = \log(C) + m\log(\Delta K_I)$ with m as the slope of the linear function. According to the Paris law, there is a single value relationship between the fatigue crack growth rate, $da/dN$and the cyclic stress intensity factor range, ΔK_I. However, some researchers have shown that the fatigue crack growth rate depends on the geometry and loading conditions of cracked specimens [2], [3], [4]. The specimen geometry is considered to act as the constraining effect on the fatigue crack growth. Therefore, various cracked specimens correspond to different levels of constraint often quantified by the T-stress values [3].

The significance of crack tip constraint for fatigue crack growth has been scarcely studied. Hutar et al. [3] suggested a phenomenological approach obtained from the assumption of linear elastic fracture mechanics (LEFM) to predict the fatigue crack growth rate under small scale yielding conditions. The model is expressed by means of two parameters, the stress intensity factor K_I and the T-stress. They discussed about the size and the shape of the plastic zone in this fatigue model and showed that both depend on the values of stress intensity factor K_I and the T-stress. Seitl and Knesl [5] used this fatigue model to study the influence of constraint on the fatigue crack growth rate in a tensile specimen with holes under mixed mode loading. Also, Roychowdhury et al. [6], [7] studied the effects of T-stress on fatigue crack closure under small scale yielding conditions. Later, Shlyannikov [8] showed that the direction and the path of fatigue cracks can be influenced strongly by both the T-stress and the SIFs. Kravchenko et al. [9] made use of a stress-based model and two-parameter fracture mechanics to study fatigue crack growth in PMMA. In their work, the effect of the higher order non-singular terms of stress on fatigue crack behavior has been investigated both theoretically and experimentally.

Sih and Barthelemy [10] suggested the strain energy density (SED) factor approach to predict the fatigue crack growth rate in order to overcome some of the shortcomings of the Paris law. Then, they used this energy- based model to analyze the effect of weld size on the path of crack growth and the fatigue life of welded cruciform joints failing from the root region [11], [12].

Lazzarin and his co-authors [13] proposed another energy-based model called the averaged strain energy density (ASED) criterion which utilizes the deformation energy averaged over a given finite-size volume surrounding the highly stressed regions. When the notch is blunt, the control area assumes a crescent shape. In crack or sharp V-notch problems, the control volume has a circular or a circular sector shape,

respectively. This energy-based model has been widely used to predict the fatigue behavior of welded joints under high cycle fatigue loading and also the fracture behavior of U- and V-shape notched specimens made of various brittle materials subjected to static loading [14], [15], [16].
Based on the previous experimental studies, the specimen geometry and boundary conditions have significant effects on the growth rate and the path of fatigue cracks in cracked components and structures. In this paper, the fatigue crack growth rate and the fatigue life of Al 7075-T6 samples have been investigated experimentally and theoretically for three different cracked specimens under pure mode-I cyclic loading. Al 7075 is a well-known high strength aluminum alloy in the grade 7xxx which is often used with various heat treatments such as T6 and T651.The experimental results are estimated theoretically using a modified ASED criterion in which the effect of T-stress as a key parameter, is taken into account in calculating the averaged strain energy density around the crack tip. It is shown that the modified criterion can predict the fatigue crack growth rate and the number of elapsed cycles of the pre-cracked specimens well.

2. Experiments

2.1. Material

The effect of specimen geometry on fatigue crack growth is studied in this research using aluminum alloy Al 7075-T6. The tensile tests were performed according to ASTM E8[17] and the yield strength σ_{ys}, the ultimate strength σ_{us} and the elastic modulus E were determined as σ_{ys} = 415 MPa, σ_{us} = 488 MPa and E = 71.7 MPa. The Poisson's ratio was taken to be 0.33 [18]. The engineering stress-strain curves for the tested Al 7075-T6 are shown in Fig. 1and its chemical composition are also presented in Table 1.

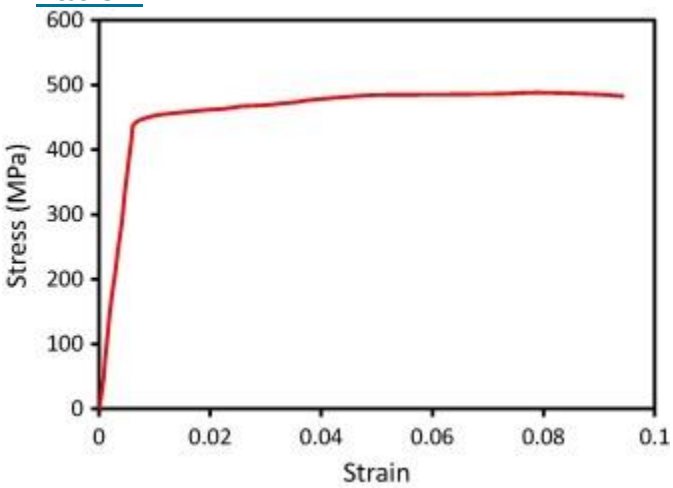

1. Download high-res image (79KB)
2. Download full-size image

Fig. 1. The engineering stress-strain curve for the tested Al 7075-T6.

Table 1. Chemical composition of Al 7075-T6 [19].

Component	Si	Fe	Cu	Mn	Mg	Zn	Ni	Cr	Pb	Sn	Ti
Weigth (%)	0.06	0.32	1.72	0.03	2.44	4.63	0.004	0.2	0.002	0.001	0.037
Component	B	Cd	Bi	Ca	P	Sb	V	Zr	Co	Li	Al
Weigth (%)	0.001	0.001	0	0.001	0.001	0.001	0.007	0.017	0.003	0.001	90.5

2.2. Test specimens

Three specimens of different shapes were considered to show the effect of specimen geometry on the results of fatigue test. As shown in Fig. 2, the test specimens were the compact tension (CT) specimen (width of W = 30 mm, height of h = 32 mm), the double cantilever beam (DCB) specimen (width of W = 60 mm, height of h = 32 mm) and the Brazilian disc (BD) specimen (radius of R = 35 mm), all with a constant thickness (t) of 12.5 mm. To check the repeatability of the tests, for each specimen, three samples were tested.

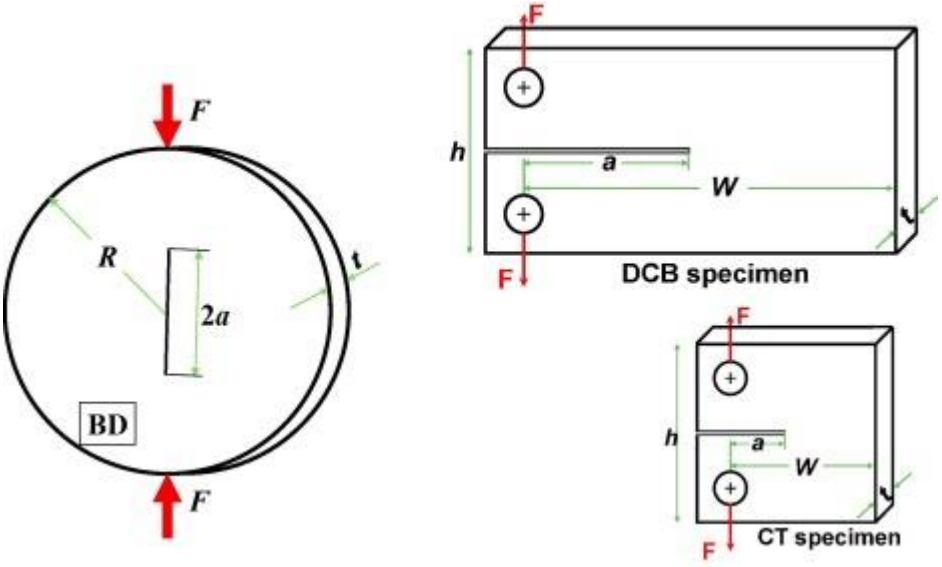

1. Download high-res image (159KB)
2. Download full-size image

Fig. 2. Three types of specimens used for fatigue crack growth experiments.

For creating the cracks, a high-precision 2D CNC water jet cutting machine was used to create a notch with an initial depth slightly less than a/W = 0.3 in the CT and DCB specimens and a/R = 0.45 in the BD specimen. Then, notched samples were pre-

loaded and pre-cycled until fatigue pre-crack formations were seen and the final crack length of each specimen was equal to a/W = 0.3 in the CT and DCB specimens and a/R = 0.45 in the BD specimen.

Load control cyclic tension tests (i.e. constant ΔF test) were performed by a servo hydraulic machine (Roell Amsler, Germany) at room temperature with loading frequency of 7 Hz (420 cycles/min). The minimum/maximum load ratio, R, was 0.1 and the applied cyclic form was sinusoidal. The maximum applied loads in these high cycle fatigue experiments were 2.40 kN, 2.20 kN and 30 kN for the CT, DCB and BD specimens, respectively. Crack growthwas monitored visually at different intervals using a digital camera (Canon EOS 600D with an EF 100 mm f/2.8 Macro Lens). Crack size, a, was measured as a function of elapsed cycles, N, and the rate of crack growth was determined by using secant method, as recommend in ASTM E647[20].

The secant technique for computing the fatigue crack growth rate simply involves calculating the slope of the straight line connecting two adjacent data points on the a versus N curve. Fig. 3 shows for example the Brazilian disc (BD) specimen before and after the fatigue experiments.

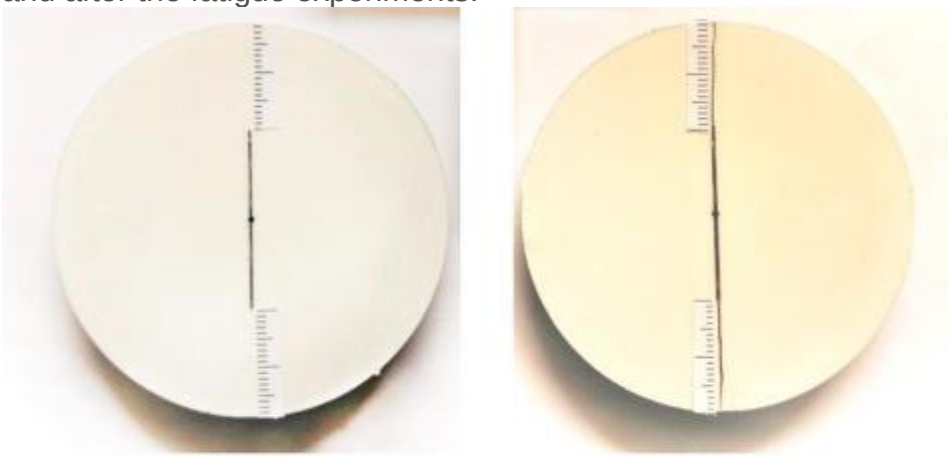

1. Download high-res image (40KB)
2. Download full-size image

Fig. 3. The Brazilian disc (BD) specimen before (a) and after (b) the high cycle fatigue experiments.

3. Fatigue crack growth model

3.1. Stress field in the neighborhood of crack tip

The elastic stress field around the crack tip in a linear elastic homogeneous and isotropicmaterial can be expressed as a set of infinite series expansions [21]. By

considering the first two terms in the Williams' expansion, the elastic stress field around the crack tip under mode I loading can be expressed as

$$\sigma_{rr}=\frac{K_I}{2\pi r}\cos\frac{\theta}{2}\left(1+\sin^2\frac{\theta}{2}\right)+T\cos^2\theta+O(r^{1/2})$$

(2)$$\sigma_{\theta\theta}=\frac{K_I}{2\pi r}\cos\frac{3\theta}{2}+T\sin^2\theta+O(r^{1/2})$$

$$\sigma_{r\theta}=\frac{K_I}{2\pi r}\cos\frac{\theta}{2}\sin\theta-T\sin\theta\cos\theta+O(r^{1/2})\sigma_{zz}=\nu(\sigma_{rr}+\sigma_{\theta\theta})\text{For plane strain}\sigma_{zz}=0\text{For plane stress}$$

where σ_{rr}, $\sigma_{\theta\theta}$, σ_{zz} and $\sigma_{r\theta}$ are the stresses in the polar co-ordinate system and (r,θ) are the polar coordinates with the origin located at the crack tip. K_I is the mode-I stress intensity factor and T is the first non-singular term and independent of distance r from the crack tip. In Eq. (2), ν is the Poisson's ratio. Crack parameters K_I and T-stress are generally dependent on the geometry and loading conditions in the cracked specimen. The higher order non-singular terms $O(r^{1/2})$ are often negligible very close to the crack tip.

3.2. Cyclic averaged elastic deformation energy range

The strain energy density concept is used in this paper for predicting the fatigue crack growth rate in isotropic materials. In plane elasticity, the strain energy density factor Saround the crack tip can be expressed in terms of the stress component as

(3)$$S=\frac{dW}{dA}=r\frac{2G\kappa+1}{8}(\sigma_{rr}+\sigma_{\theta\theta})^2-\sigma_{rr}\sigma_{\theta\theta}+\sigma_{r\theta}^2$$

where dW/dA is the strain energy density function and G is the shear modulus. It is known that $G=E/2(1+\nu)$ in which E is the modulus of elasticity. κ is defined as $3-4\nu$ in plane strain and $\frac{3-\nu}{1+\nu}$ in plane stress problems. By substituting the crack tip stresses from Eq. (2)into Eq. (3) and manipulating the resulting expressions, one may write the strain energy density function as

(4)$$\frac{dW}{dA}=S_r=\frac{1}{16\pi r}\left[a_1K_I^2+a_2\sqrt{2\pi r}K_IT+a_3(2\pi r)T^2\right]$$

in which

(5)$$a_1=(\kappa-\cos\theta)(1+\cos\theta)\quad a_2=\cos\theta\left[\cos(2\theta)-\cos\theta+(\kappa-1)\right]\quad a_3=(\kappa+1)^2$$

The elastic deformation energy within the circular region of area A and radius r_c around the crack tip (Fig. 4) is written as

(6)$$E(r_c)=\int_A dW\,dA\,dA=\int_0^{r_c}\int_{-\pi}^{\pi}\frac{dW}{dA}r\,dr\,d\theta=N_1K_I^2+N_2K_IT+N_3T^2$$

in which

(7)$$N_1=\frac{(2\kappa-1)r_c}{16G}\quad N_2=\frac{2r_c^3}{2(5\kappa-7)}\quad N_3=\pi r_c^2\frac{(\kappa+1)}{16G}$$

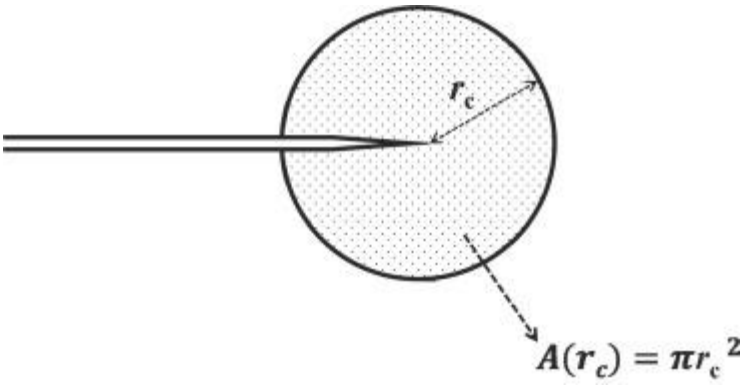

1. Download high-res image (92KB)
2. Download full-size image

Fig. 4. The critical area around the crack tip.

Therefore, the elastic deformation energy, averaged over the area $A(r_c)$, turns out to be:

(8)E¯=E(rc)A(rc)=1πrc2[N1KI2+N2KIT+N3T2]

The cyclic averaged elastic deformation energy range $\Delta\bar{E}$ under the maximum and minimum loads during one cycle follows the equation

(9)ΔE¯=E¯max-E¯min

where E¯max and E¯min are the maximum and the minimum values of the averaged elastic deformation energy corresponding to the maximum load and minimum load during one cycle, respectively.

(10)E¯max=E¯(σmax),E¯min=E¯(σmin)

By replacing the averaged elastic deformation energy from Eq. (8) into Eq. (9) and simplifying the obtained equation, one may derive:

(11)ΔE¯=E¯max-E¯min=1πrc2[2N1K¯IΔKI+N2(K¯IΔT+T¯ΔKI)+2N3T¯ΔT]

where ΔK_I and ΔT are defined as the cyclic stress intensity factor range and T-stress range, respectively. Also K¯I and T¯ are the mean stress intensity factor and mean T-stress, respectively. These parameters are defined as

(12)K¯I=(KI)max+(KI)min2ΔKI=(KI)max-(KI)minT¯=(T)max+(T)min2ΔT=(T)max-(T)min

It is common to show the T-stress and the radius of control volume r_c by two dimensionless parameters of biaxiality ratio B[22] and α as

(13)B=Tmaxπa(KI)max=Tminπa(KI)minandα=2rca

where a is the semi-crack length for center cracks and the crack length for edge-cracks. By using the parameters B and α, Eq. (11) can be rewritten in terms of $B\alpha$ as

(14)ΔE¯=E¯max-E¯min=(1-R2)(KI)max216πrcG[(2κ-1)+16(5κ-7)15π(Bα)+(κ+1)2(Bα)2]

where R is the minimum/maximum cyclic load ratio ($R=(KI)min/(KI)max=Tmin/Tmax$). If the terms containing the T-stress in Eq. (14) vanish, the cyclic averaged elastic deformation energy range (ΔE^{-}) can be written as

(15)$\Delta E^{-}0=E^{-}max-E^{-}min=(1-R2)(KI)max2(16\pi rcG)(2\kappa-1)$

3.3. Fatigue crack growth rate

Since the elastic deformation energy over control volume around the crack tip is based on the concept of the strain energy density, the relation between da/dN (for midrange fatigue crack growth rate) and ΔE^{-} can be described by a power function. Hence, the relation can be defined the in the same way as that of the energy-based model suggested by Sih and Barthelemy [10].

(16)$dadN=P(\Delta E^{-})u$

where P and u are the material constants obtained for the conditions corresponding to T = 0. By including the effect of T-stress in ΔE^{-} (Eq. (14)), the influence of changing constraint level on the fatigue crack growth rate is considered. In the generalized ASED (GASED) criterion, the value of the cyclic averaged elastic deformation energy range ΔE^{-} in Eq. (16)is calculated by using Eq. (14) which considers the effect of T-stress while the value of $\Delta E^{-}$is determined by using Eq. (15) in the conventional ASED criterion.

4. Results and discussion

A numerical subroutine was developed in which the crack growth is simulated for three specimens described in Section 2.2 i.e. the CT, DCB and BD specimens. The numerical subroutine was then linked to the finite element code ABAQUS to calculate the values of SIF and T-stress required for the specimens in every incremental length of crack growth. The elastic material properties of Al 7075-T6 mentioned earlier were considered in finite element modeling. Considering the relatively large value of thickness with respect to the other dimensions, plane strain conditions were assumed. Isoparametric 8-node quadrilateral elements were used to mesh the models of specimens. Singular elements were considered in the first ring of elements (next to the crack tip) for producing the square root singularity of the strain/stress field. An interaction integral method built in ABAQUS [23] was used for obtaining the crack tip parameters (SIF and T-stress) directly. The biaxiality ratio B in each length of crack was determined using the equation $B=T\pi aKI$ which shows the ratio of the T-stress relative to the stress intensity factor. Fig. 5 shows the variations of the biaxiality ratio B with crack growth length in the CT, DCB and BD specimens.

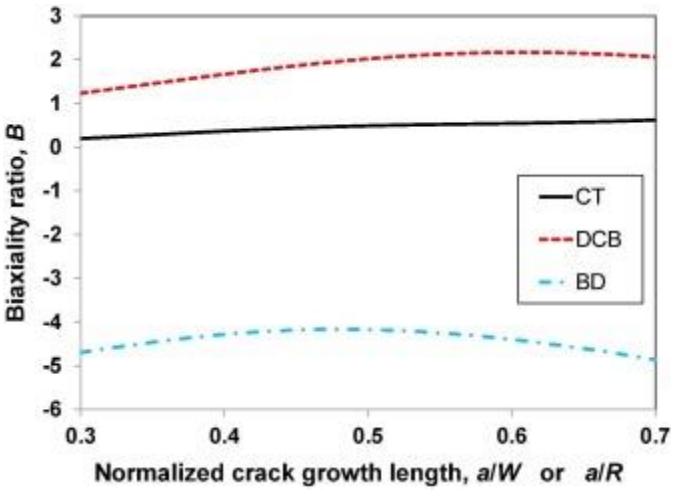

1. Download high-res image (109KB)
2. Download full-size image

Fig. 5. Variations of biaxiality ratio (B) with the crack length for the CT, DCB and BDspecimens.

It is seen from Fig. 5 that the value of B (and hence T-stress) in the BD specimen is significantly negative while it is positive for the DCB specimen and its magnitude is very small for all the crack lengths in the CT specimen.

By using Eq. (14), the cyclic averaged elastic deformation energy range during one cycle under mode I loading at a given distance from a crack tip, x, can be shown to be:

(17)$$\Delta\bar{E}(x)=\bar{E}\max(x)-\bar{E}\min(x)=(1-R2)(KI)\max 2(16\pi xG)(2\kappa-1)+16(5\kappa-7)15\pi B2xa+\kappa+12B22xa$$

The contribution of the T-stress in the value of the averaged elastic deformation energy at a given distance from the crack tip, x, is presented here by dimensionless parameter $\Lambda(x)$. This parameter is calculated by dividing the value of the cyclic averaged elastic deformation energy range without T-stress term ($\Delta\bar{E}0(x)$) by the cyclic averaged elastic deformation energy range which includes the T-stress term ($\Delta\bar{E}(x)$) and is defined as

(18)$$\Lambda(x)=\Delta\bar{E}0(x)\Delta\bar{E}(x)=11+B2xa16(5\kappa-7)15\pi(2\kappa-1)+(\kappa+1)2(2\kappa-1)B22xa$$

The variations of the parameter $\Lambda(x)$ versus the normalized distance ahead of the crack tip, x/a_0, (a_0 is initial crack length) are shown in Fig. 6 for different samples when v = 0.33. It can be seen from this figure that for all the specimens the value of $\Lambda(x)$ starts at unity and then decreases as the distance from the crack tip increases. $\Lambda(x)$ drops faster or slower depending on the type of specimen. Since the value of T-stress is negligible in comparison with the value of SIF in the CT specimen (see Fig. 5), the variations of the parameter $\Lambda(x)$ with the increase in distance from the crack tip is

negligible and hence, $\Lambda(x)$ is close to the unity. However, in the DCB and BD specimens, $\Lambda(x)$ changes significantly with the increase in the distance from the crack tip. In other words, the contribution of the nonsingular component (T-stress) in calculating the averaged strain energy density around the crack tip in the DCB and BD samples is much higher than that of the CT one. Eq. (18) is a function of two parameters x/a and B such that both simultaneously affect $\Lambda(x)$. The parameter x could be replaced by the radius of control volume r_c which is a material property. Fig. 7 displays the variations of the parameter $\Lambda(r_c)$ versus $B\alpha=T_{max}2\pi r_c(K_I)_{max}$. As can be seen from this Figure, the parameter $\Lambda(r_c)$ is considerably dependent on the T-stress (or $B\alpha$) in a way that by increasing the absolute value of $B\alpha$, the parameter $\Lambda(r_c)$ reduces.

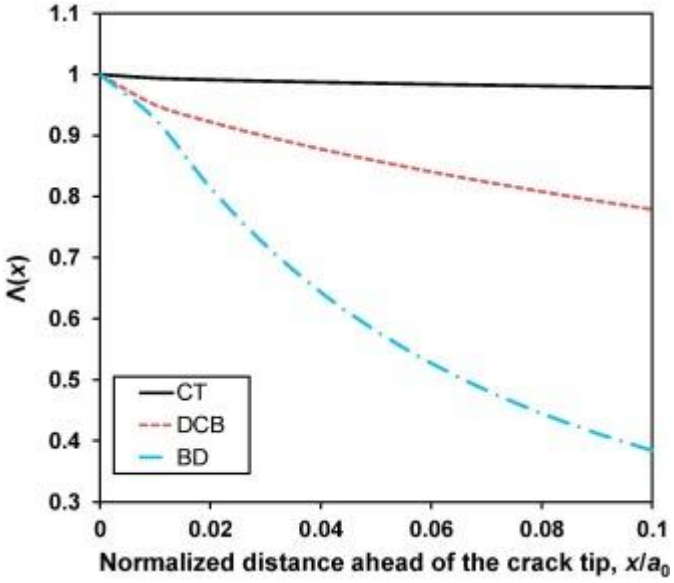

1. Download high-res image (122KB)
2. Download full-size image

Fig. 6. Variations of the parameter $\Lambda(x)$ versus the normalized distance ahead of the crack tip, x/a_0 for CT, DCB and BD specimens.

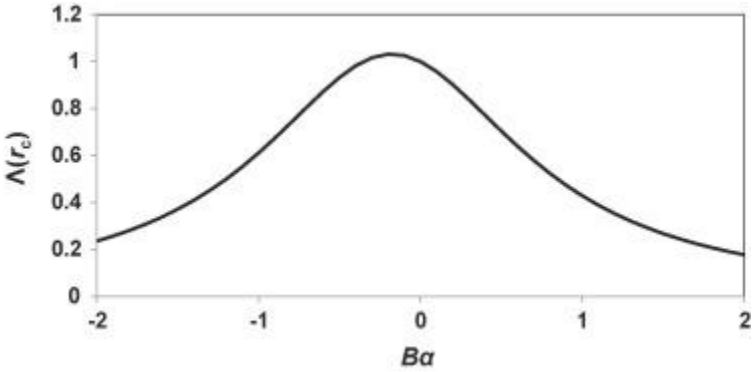

1. Download high-res image (56KB)
2. Download full-size image

Fig. 7. Variations of the parameter $\Lambda(r_c)$ for different values of $B\alpha$ (v = 0.33).

The size of control volume radius around the crack tip can be estimated based on a theoretical model proposed by Seweryn [24]:

(19)$rc=2\pi KIc\sigma ys2$

where K_{Ic} is the mode-I fracture toughness. By replacing the values of K_{Ic} = 18.75 MPa $m^{0.5}$and σ_{ys} = 415 MPa obtained from our experiments performed on Al 7075-T6, Eq. (19) gives r_c = 1.3 mm. Lazzarin et al. [13] also used the same model to predict the size of control volume radius for samples made of Duraluminium.
In this investigation, the material constants *P* and *u* in Eq. (16) are determined from the results of high cycle fatigue experiments on the CT specimen in which the T-stress (or *B*) is negligible. Then, Eqs. (14), (16) are used to predict the fatigue crack growth rate and the number of elapsed cycles of the DCB and BD specimens in high cycle fatigue region. More details are given in the forthcoming sections.

4.1. Material fatigue constants

Fatigue crack growth rates were measured for AL 7075-T6 alloy using the CT specimen. Fig. 8 shows the fatigue crack propagation rate data versus the cyclic averaged elastic deformation energy range. For any desired fatigue crack length, the value of the cyclic averaged elastic deformation energy range was calculated by using Eq. (14). For the CT specimen, a linear relation was found between the fatigue crack propagation rate, d*a*/d*N*, and the cyclic averaged elastic deformation energy range, ΔE^{-} in a logarithmic scale. The linear regression analysis was used to determine the material fatigue constants. Table 2gives the values of the constants *P* and *u* in Eq. (16). The constants *P* and *u* given in Table 2describe the median curve approximating the experimental data points at crack growth rates for the CT specimen of Al 7075-T6.

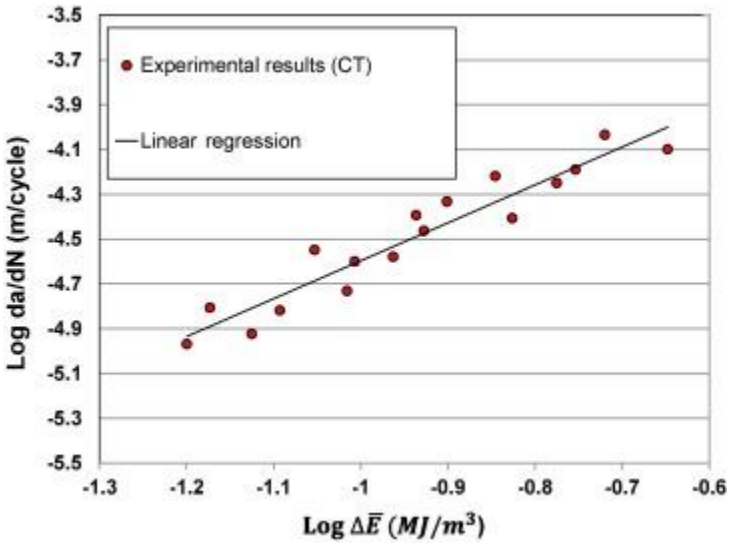

1. Download high-res image (131KB)
2. Download full-size image

Fig. 8. Fatigue crack growth rate data for the CT specimens made of Al 7075-T6 alloy.

Table 2. Experimental constants in Eq. (16) obtained for the CT specimen made of Al 7075-T6 alloy [d*a*/d*N*] = m/cycle; [ΔE^{-}] = MJ/m^3.

Sample	***P***	***u***
CT	1.69	0.0013

4.2. DCB and BD specimens

Pin-loading fixture was utilized throughout the fatigue testing in the DCB specimens. The external load was applied via two pin holes designed on the DCB sample. The fatigue testswere conducted on the BD specimens using two flat loading disks as shown in Fig. 9. Mode I is provided in this specimen, when the crack line is oriented parallel to the loading direction.

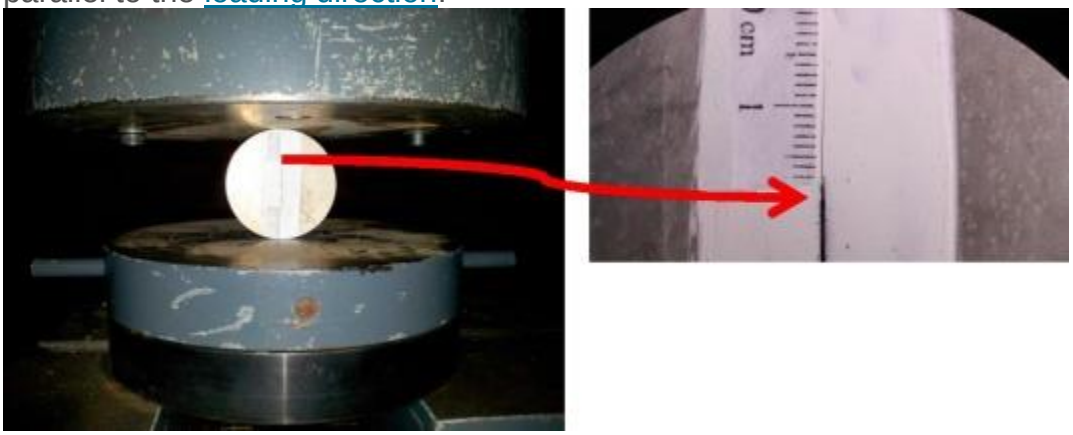

1. Download high-res image (75KB)

2. Download full-size image

Fig. 9. Loading set up used for the BD specimen.

The numbers of elapsed cycles, N, in the CT and BD specimens were calculated by using the generalized energy-based model (GASED criterion) proposed in this paper. To predict the number of elapsed cycles in a cracked specimen, first the cyclic averaged elastic deformation energy range at the crack tip should be determined. By substituting the numerical values of K_I and T-stress obtained in each incremental length of crack growth into Eq. (14), the cyclic averaged elastic deformation energy range ΔE^- can be determined from the GASED criterion. Afterwards, the number of elapsed cycles, N, in each incremental length of crack growth was calculated by using the equation $\Delta N=\Delta a P(\Delta E^-)u$ and the material fatigue constants (P and u) presented in Table 2. A constant incremental length of crack growth (Δa = 0.5 mm) was considered in every computation step. For the sake of comparison, the conventional ASED criterion was also employed to predict the number of elapsed cycles by using the cyclic averaged elastic deformation energy range without considering the effect of the T-stress (Eq. (15)). Fig. 10, Fig. 11 show the experimental results and the theoretical predications based on the GASED criterion and the conventional ASED criterion in terms of the number of elapsed cycles in the DCB and BD specimens made of Al 7075-T6 alloys, respectively. It is seen from Fig. 10, Fig. 11 that the GASED criterion provides more accurate predications than the conventional ASED criterion for the experimentally determined elapsed cycles of Al 7075-T6 alloys.

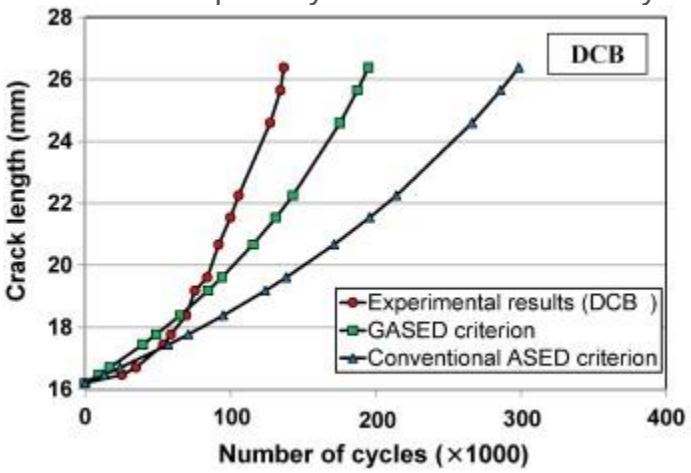

1. Download high-res image (154KB)
2. Download full-size image

Fig. 10. Predictions of the GASED and conventional ASED criteria for the number of elapsed cycles of Al 7075-T6 alloys obtained by using the DCB specimen.

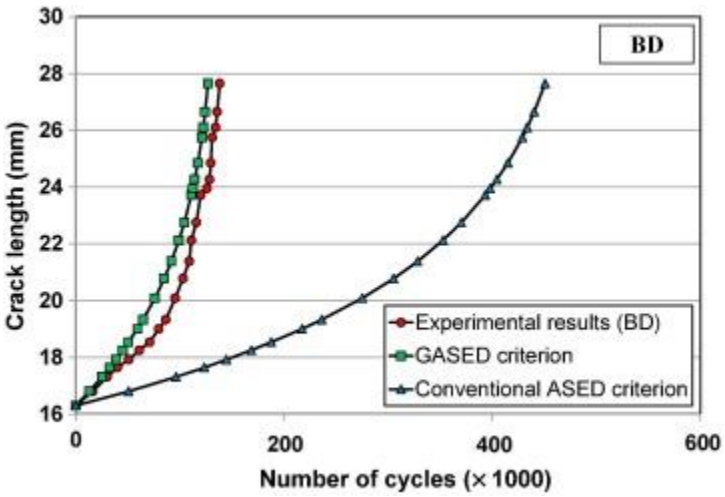

1. Download high-res image (158KB)
2. Download full-size image

Fig. 11. Predictions of the GASED and conventional ASED criteria for the number of elapsed cycles of Al 7075-T6 alloys obtained by using the BD specimen.

Fig. 12 displays the fatigue crack propagation rate data versus the cyclic averaged elastic deformation energy range when considering the effect of T-stress in the CT, DCB and BD specimens. The experimental data obtained from the CT, DCB and BD specimens are predicated by using the GASED criterion based on Eqs. (14), (16). According to Fig. 5, the absolute values of T-stress in the DCB and BD specimens are significant. Accordingly, T-stress plays an important role in calculating the value of the averaged strain energy density around the crack tip and in deriving the curve of fatigue crack growth rate based on the proposed energy-based model. It is seen in Fig. 12 that the material fatigue constants obtained from high cycle fatigue experiments on the CT specimen which has a negligible T-stress can be used to predict the fatigue crack growth rate in the DCB and BD specimens. It is also concluded that the GASED criterion could provide good predictions for the fatigue crack growth rate in the tested specimens in a wide range of fatigue crack lengths and for specimens with both positive and negative T-stresses. Fig. 13 illustrates the fatigue crack growth rate data obtained from the experiments together with the theoretical predications of the conventional ASED criterion. It is seen that the conventional ASED criterion which makes use of only the first term in the Williams' series expansion (Eq. (15)) fails to predict the fatigue crack growth rate obtained from fatigue tests on the DCB and BD specimens.

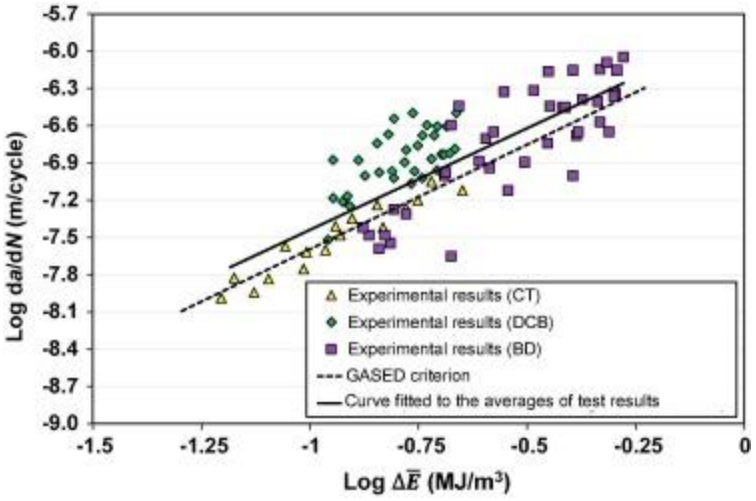

1. Download high-res image (197KB)
2. Download full-size image

Fig. 12. The predicted fatigue crack growth behavior in the CT, DCB and BD specimens based on the GASED criterion.

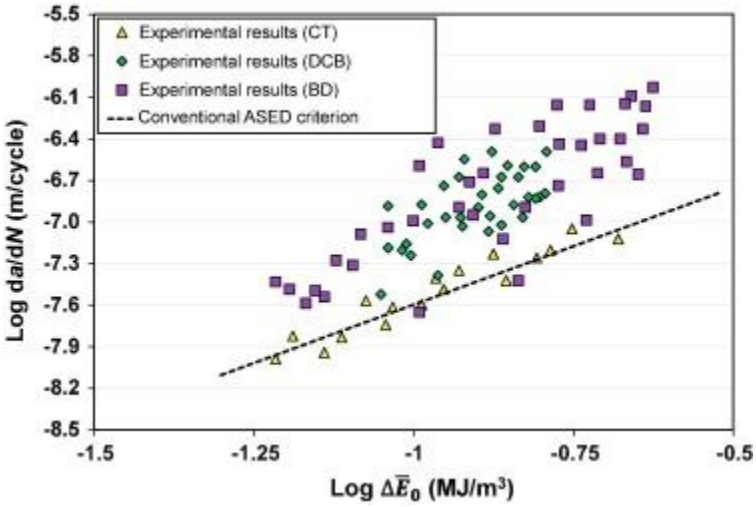

1. Download high-res image (171KB)
2. Download full-size image

Fig. 13. The predicted fatigue crack growth behavior in the CT, DCB and BD specimens based on the ASED criterion.

5. Conclusions

The averaged strain energy density criterion was modified and then employed to predict the fatigue crack growth rate and the number of elapsed cycles in each incremental length of crack growth in the CT, DCB and BD specimens made of Al 7075-T6 alloys

under mode-I fatigue loading. The main findings of this research are summarized as follows:

1. The crack tip parameters K_I and T-stress were calculated for the CT, DCB and BD specimens in each incremental length of crack growth using a large number of finite element analyses. It was found that the magnitudes of T-stress in either of the DCB and BD test specimens are significant and affect the value of the averaged strain energy density around the crack tip.
2. There was a significant discrepancy between crack growth curve predicted by using the conventional ASED criterion and the experimental results obtained from the DCB and BD specimens.
3. The GASED criterion which considers the effect of *T*-stress in addition to the singular term could provide good estimates for the experimentally determined fatigue crack growth rate and for the elapsed cycles both in a positive T-stress specimen (DCB) and in a negative T-stress specimen (BD).